Biomass and Bioenergy 209 (2026) 108920

Contents lists available at ScienceDirect

Biomass and Bioenergy

journal homepage: www.elsevier.com/locate/biombioe

Kaolin additivation in pulverized wood firing systems – potassium capture, emissions and ash behavior

Theresa Siegmund *, Marvin Scherzinger, Martin Kaltschmitt

Institute of Environmental Technology and Energy Economics, Hamburg University of Technology (TUHH), Eissendorfer Strasse 40, 21073, Hamburg, Germany

ARTICLE INFO

Keywords:
Pulverized fuel
Combustion
(Fuel) additivation
Kaolin
Ash fusion
Emissions

ABSTRACT

Pulverized fuel (PF) combustion systems based on solid biofuels are a key in sustainable energy transition, especially when retrofitting coal-fired plants. Nonetheless, challenges persist due to alkali metal-induced emissions and ash-related operational issues. This paper investigates the effect of kaolin additivation during pulverized biomass combustion. Industrial wood pellets were milled and mixed with kaolin at concentrations of 0.5, 1.0, and 1.5 wt% and combusted in a laboratory-scale PF furnace. Prior laboratory analyses showed that 1.5 wt% kaolin additivation increased potassium retention in ashes from 34 % to 96 % at 1100 °C and raised ash fusion temperatures (e.g., flow temperature from 1277 °C to 1432 °C), indicating the formation of high temperature-stable potassium(K)-aluminum(Al)-silicate compounds. Combustion tests revealed alterations in gaseous emissions (nitrogen oxides (NO_x) and carbon dioxide (CO_2)) as well as changes in the composition of the resulting ashes. Chemical and X-ray diffraction analyses suggest a shift of potassium compounds within the ash fractions and a formation of stable K-Al-silicate compounds within the bottom ash. However, high ignition losses were reported for the bottom ashes, attributable to incomplete combustion linked to short residence times. This was also reflected in high CO emissions, which did not show a significant improvement with additivation. Although the results from the PF combustion experiments do not allow a generalization of emissions trends due to incomplete burnout, the observed trends, along with laboratory results, confirm and highlight the potential of kaolin as an additive to mitigate K-related detrimental effects in PF biomass combustion systems.

1. Introduction

The use of biomass for electricity and heat generation has played—and will likely continue to play—a vital role in "green" energy provision. In large-scale applications, combustion technologies for solid biofuels include grate firing (GF), fluidized bed (FB), and pulverized fuel (PF) systems. The latter is significant for retrofitted coal-fired power plants, facilitating the transition to biomass-based fuels as part of the shift toward green energy, enabling operation at up to 600 MW_e [1].

The conversion of pulverized fuel plants from the fuel coal to the fuel biomass presents several challenges. This includes, primarily due to the chemical composition of biomass fuels compared to coal, slagging due to low melting compounds in the ash [2], corrosion caused by high combustion temperatures, e.g., due to elevated chlorine (Cl) content, as well as the risk of high-dust $DeNO_x$ poisoning due to alkali metals such as potassium (K) and sodium (Na) [3]. One possibility to mitigate these detrimental effects is using fuel additives. Kaolin, a widely assessed option [4], is an aluminum-silicate-based mineral primarily composed of kaolinite $Al_2Si_2O_5(OH)_4$. This mineral reacts under the conditions given within the combustion zone and binds alkali metals (i.e., particularly K) into high-temperature-stable compounds, which are retained in the bottom ash. When introduced into the combustion chamber, kaolinite undergoes reactions as depicted in equation (1) for temperatures above 450 °C, equation (2) for temperatures at 980 °C and equation (3) for temperatures above 1100 °C [5].

$$Al_2Si_2O_5(OH)_4\ (\text{kaolinite}) \rightarrow Al_2O_3{\cdot}2SiO_2\ (\text{meta-kaolin}) + 2H_2O \quad (1)$$

$$Al_2O_3{\cdot}2SiO_2\ (\text{meta-kaolin}) \rightarrow Al_2O_3{\cdot}SiO_2\ (\text{spinel}) + SiO_2 \quad (2)$$

$$3(Al_2O_3{\cdot}SiO_2)\ (\text{spinel}) + 3SiO_2 \rightarrow 3Al_2O_3 \cdot 2SiO_2\ (\text{mullite}) + 4SiO_2 \quad (3)$$

Studies with residence times of 1.2 s have shown that only a fraction of kaolinite is converted to mullite, with the majority remaining as amorphous meta-kaolin and spinel [6]. Thus, the primary reaction products formed during the calcination of kaolin subsequently interact

* Corresponding author.
E-mail address: theresa.siegmund@tuhh.de (T. Siegmund).

https://doi.org/10.1016/j.biombioe.2025.108920
Received 23 September 2025; Received in revised form 20 November 2025; Accepted 30 December 2025
Available online 10 January 2026

with gaseous alkali species [5]. Equation (4) till (6) illustrate, in a simplified manner, the transformation of meta-kaolin into kalsilite or kaliophilite ($KAlSiO_4$). The formation of leucite ($KAlSi_2O_6$) and orthoclase ($KAlSi_3O_8$) follows a similar pathway to orthoclase but involves the incorporation of additional SiO_2 molecules.

$$Al_2O_3{\cdot}2SiO_2 + 2KCl + H_2O \rightarrow 2KAlSiO_4 + 2HCl \quad (4)$$

$$Al_2O_3{\cdot}2SiO_2 + K_2SO_4 \rightarrow 2KAlSiO_4 + SO_3 \quad (5)$$

$$Al_2O_3{\cdot}2SiO_2 + 2KOH \rightarrow 2KAlSiO_4 + H_2O \quad (6)$$

These reactions suppress the release of volatile, gaseous K-compounds such as KOH, KCl, and K_2SO_4, which may result in.

- Increased bed ash stability due to the formation of compounds with high melting temperatures [2,7],
- mitigation of inorganic particulate matter (PM) emissions [8–13], and
- lower CO emissions in the flue gas [14–16].

While these effects of kaolin additivation have been drawn mainly in studies in grate firing (GF) systems, the effects of kaolin in PF furnaces remain largely unexplored. Fuller et al. [12] investigated the effects of an "aluminum-silicate additive" on wood fly ash in a lab-scale pulverized fuel reactor. They found that additivation not only reduced K, Fe, Ca, Mg, and Na compounds but also led to lower concentrations of Cr and soluble Cr(VI) compounds in the fly ash. Similar findings were reported by Delgado et al. [17] in a study with a 120 kW_{th} pulverized fuel pilot plant, where coal fly ash (rich in Si and Al) was added to the combustion process, and pilot-scale data were compared with full-scale experiments in commercial power plants. In this pilot plant, PM_1 emissions (i.e., particulate matter with an aerodynamic diameter <1 μm) were lowered by 32 %, while the concentrations of K, Na, S, and Cl in the PM emissions were reduced considerably. Full-scale experiments have been conducted in two power plants in Denmark.

- In Avedøre Power Station (800 MW_{th}) [17–19], coal fly ash was introduced via combustion air, resulting in fly ash dominated by spherical particles rich in Si and Al, and significantly reducing concentrations of K-containing species (i.e., KCl, K_2SO_4, and KOH). Additionally, negligible amounts of K_2SO_4 on heat exchanger surfaces [18], and a decrease in PM_1 emissions by 36 % were reported.
- In Studstrup Power Station (900 MW_{th}), coal fly ash was added as a slurry to the pellet mill. This additivation led to the incorporation of K, resulting in a 43 % reduction in PM_1 emissions [17].

Against the lack of investigations of kaolin additivation in PF furnaces and the influence on K capture and gaseous emissions, this study combines laboratory-scale analyses with experiments in a pilot or laboratory-scale pulverized fuel furnace to evaluate the transferability of results obtained under idealized conditions to more realistic combustion scenarios. Laboratory tests with milligram to gram fuel quantities enable a systematic investigation of the chemical interactions and formation mechanisms of stable potassium-aluminum-silicate compounds under controlled conditions. These settings, however, do not capture the reaction kinetics, flow behavior, particle size distributions, and residence times typical for technical combustion systems, whether in pilot or industrial scale. By comparing laboratory analysis methods with laboratory combustion experiments, the study examines the practical relevance of laboratory findings for their transferability to pulverized biomass combustion, e.g., to estimate an optimal additive content for this additive/fuel combination.

2. Materials and methods

The experiments included laboratory analyses and combustion tests in a PF furnace. Milled industrial wood pellets were used as the solid biofuel, with kaolin added at concentrations of 0.5, 1.0, and 1.5 wt% (e.g., 150 g kaolin added for 15 kg material for the 1.0 wt% condition). The resulting molar ratios of Al:Si:K provide sufficient theoretical excess of Al and Si for complete incorporation of K into the ash (cf. Table 3 below). The material was mixed in a concrete mixer for 10 min. Additive concentrations were selected based on prior experiments with wood in GF systems [20,21] and literature on PF systems with coal ash and aluminum-silicate-based additives [12,17,19,22]. Laboratory analyses of the mixtures included measurements of ash fusion temperatures, ash content at 550 °C, and potassium (K) retention of 1100 °C ashes compared to 550 °C ashes, both with and without additive (section 2.3). Following the laboratory tests, combustion experiments were conducted in a PF furnace (section 2.4). Online measurements of gaseous emissions (i.e., CO_2, CO, NO, NO_2, SO_2, and O_2) were performed (section 2.4.1). Ash samples (i.e., bottom ash, cyclone ash, and filter ash from combustion) were collected and thereafter analyzed to determine both the chemical composition and the crystalline phases as evidence for the formation of K and kaolin reaction products (sections 2.4.2 till 2.4.4).

2.1. Solid biofuel: wood pellets

Wood pellets for industrial applications with fuel properties and chemical composition as specified in Table 1 were used for the laboratory and combustion experiments. Prior to mixing with the additive, the pellets were milled using a Fritsch pulverisette 16 cross-beater mill equipped with a 0.5 mm sieve, resulting in a median particle size $d_{p50\ wt\ \%}$ of 433 μm. The particle size distribution was measured using a particle size analyzer (Retsch, Camsizer XT).

2.2. Additive: kaolin

The additive was kaolin, consisting mainly of the mineral kaolinite ($Al_2Si_2O_5(OH)_4$) (supplied by Gebrüder Dorfner GmbH & Co. Kaolin-und Kristallquarzsandwerke KG). This kaolin is extracted from naturally occurring mineral deposits, with significant reserves located in the USA, China, and Germany, among others [26]. The composition of the used

Table 1
Fuel properties and chemical composition of the wood pellets (a.r. as received, d.b. dry basis) [23–25].

Parameter	Unit	Wood Pellets	Method of analysis
Moisture content	$wt\%_{a.r}$	8.0	ISO 18134-2
Ash content	$wt\%_{d.b.}$	0.9	ISO 18122
HHV	$MJ/kg_{d.b}$	20.2	ISO 18125
LHV	$MJ/kg_{d.b}$	18.7	ISO 18125
Carbon (C)	$wt\%_{d.b.}$	50.0	ISO 16948/ISO 16994
Hydrogen (H)	$wt\%_{d.b.}$	7.0	ISO 16948/ISO 16994
Oxygen (O)	$wt\%_{d.b.}$	41.7	by mass difference
Nitrogen (N)	$wt\%_{d.b.}$	0.12	ISO 16948/ISO 16994
Sulphur (S)	$wt\%_{d.b.}$	0.28	ISO 16948/ISO 16994
Calcium (Ca)	$mg/kg_{d.b.}$	1740	ISO 16967/ISO 16994
Potassium (K)	$mg/kg_{d.b.}$	941	ISO 16967/ISO 16994
Sodium (Na)	$mg/kg_{d.b.}$	110	ISO 16967/ISO 16994
Magnesium (Mg)	$mg/kg_{d.b.}$	347	ISO 16967/ISO 16994
Phosphorus (P)	$mg/kg_{d.b.}$	142	ISO 16967/ISO 16994
Manganese (Mn)	$mg/kg_{d.b.}$	101	ISO 16967/ISO 16994
Silicon (Si)	$mg/kg_{d.b.}$	636	ISO 16967/ISO 16994
Iron (Fe)	$mg/kg_{d.b.}$	147	ISO 16967/ISO 16994
Aluminum (Al)	$mg/kg_{d.b.}$	140	ISO 16967/ISO 16994
Phosphorus (P)	$mg/kg_{d.b.}$	<408	ISO 16967/ISO 16994
Zinc (Zn)	$mg/kg_{d.b.}$	14	ISO 16968
Lead (Pb)	$mg/kg_{d.b.}$	0.58	ISO 16968
Copper (Cu)	$mg/kg_{d.b.}$	10	ISO 16968
Nickel (Ni)	$mg/kg_{d.b.}$	5	ISO 16968
Chrom (Cr)	$mg/kg_{d.b.}$	8	ISO 16968
Barium (Ba)	$mg/kg_{d.b.}$	18	ISO 16968
Chloride (Cl^-)	$mg/kg_{d.b.}$	80	ISO 10304-1

kaolin is depicted in Table 2. The median particle size was $d_{p50\ wt\%} = 37$ µm.

2.3. Laboratory experiments

Laboratory analyses were conducted to evaluate the combustion properties of the additivated wood before combustion experiments in the pulverized fuel furnace. The additivated wood samples were analyzed in triplicate to assess their water content, ash content, ash retention, and K retention. To investigate the thermal degradation behavior of the additivated biomass and the gaseous species released during decomposition, evolved gas analyses were carried out using combined thermogravimetric analysis (TGA) coupled with a micro gas chromatograph (µGC). Additionally, ash fusion temperatures were investigated.

Issues such as slagging, deposit formation, and fouling during combustion are frequently linked to low ash melting temperatures, which are strongly influenced by the composition of the solid biofuel and its resulting (bottom) ash [28]. Medium to high concentrations of K and Si in ashes can form eutectics with relatively low melting points (down to 769 °C) [29]. The formation of K aluminosilicates, on the other hand, results in high-temperature-stable compounds (e.g., kalsilite ($KAlSiO_4$) or leucite ($KAlSi_2O_6$)), though these compounds are not typically present in all biomass ashes [30]. Therefore, enriching solid biofuels with mineral-based additives can enhance the formation of these high-temperature-stable compounds. Nonetheless, such a measure might have consequences such as alteration of the ash chemistry, e.g., by binding K and other alkali-elements within temperature-stable compounds (i.e., "alkali-getter-effect"), physical absorption of condensable vapors, and the dilution of problematic, low-melting species [31]. An overview of the analyzed samples, as well as the resulting Al/K and Si/K ratios from Si, Al, and K from within the biomass and from the introduced kaolin is provided in Table 3.

2.3.1. Water and ash content, ash and K retention

Water content was measured at 105 °C in a drying oven for 24 h, and the ash content was determined in a muffle furnace (Nabertherm L 24/11 BO) at 550 °C according to DIN EN 18122 standard [32]. To determine the K retention, part of the ashes produced at 550 °C were again heated from room temperature to 1100 °C in the same muffle furnace with a heating rate of ca. 10 K/min up to 550 °C, followed by a slower heating rate of 3 K/min from 550 to 1100 °C. The samples were then maintained at the final temperature for 15 min to ensure complete heat transfer within the sample. For each analysis, 100 mg of each ash sample (i.e., 550 °C and 1100 °C ash) was then digested with acid in two steps in a microwave oven (Anton Paar GmbH Microwave GO) according to DIN 22022–1 [33]. K concentrations were then measured by atomic absorption spectroscopy (AAS, Analytik Jena AG ContraAA 700). The K retention was determined using equation (10), where $c_{K@1100°C}$ and $c_{K@550°C}$ represent the K concentrations at 1100 °C and 550 °C, respectively, and $m_{ash@1100°C}$ and $m_{ash@550°C}$ denote the corresponding ash. The latter ratio of the equation indicates the ash retention.

Table 2
Composition of kaolin additive [27].

Parameter	Unit	Kaolin
SiO_2	$wt\%_{a.r.}$	50.2
Al_2O_3	$wt\%_{a.r.}$	34.4
H_2O	$wt\%_{a.r.}$	12
CaO	$wt\%_{a.r.}$	<0.1
TiO_2	$wt\%_{a.r.}$	0.4
Fe_2O_3	$wt\%_{a.r.}$	0.5
K_2O	$wt\%_{a.r.}$	2.1
Na_2O	$wt\%_{a.r.}$	0.2
MgO	$wt\%_{a.r.}$	<0.1
P_2O_5	$wt\%_{a.r.}$	0.2

Table 3
Denotation of (with kaolin additivated) wood samples used for laboratory experiments.

Sample	Addition of kaolin in wt%	Al/K in mol%	Si/K in mol%
Ref	–	0.2	0.9
K05	0.5	1.6	2.6
K10	1.0	2.7	3.9
K15	1.5	3.7	5.1

$$K_{retention} = \frac{c_{K@1100°C}}{c_{K@550°C}} \cdot \frac{m_{ash@1100°C}}{m_{ash@550°C}} \cdot 100\ \% \quad (10)$$

The retention of K demonstrates the amount of K remaining within the ash and was not released as volatile compounds (e.g., as KCl or K_2SO_4) at elevated temperatures between 550 °C and 1100 °C. Adding kaolin promotes the formation of temperature-stable K compounds within the ash, resulting in higher K retention compared to non-additivated solid fuels. Increased K retention thus correlates with lower K levels in the flue gas during the combustion of solid fuels.

2.3.2. Gas evolution from thermal degradation

Thermogravimetric analysis (TGA, Mettler Toledo, system TGA 2) was coupled with a micro gas chromatograph (µGC, Micro-GC SRA Instruments R990, with Module A: MS-5A 10 m and Module B: PoraPlot U 10 m, standard gas concentration for CO: 2 mol%, CO_2: 3 mol%) to measure the evolved gas concentrations of CO and CO_2 during TGA experiments. About 20 mg of the samples were used in a 150 µL aluminumoxide crucible; experiments were carried out in duplicates in order to validate the observed trends qualitatively. For reference, the plain additive was also analyzed. The measurements were performed under air with a gas flow of 30 mL/min and a dynamic temperature profile of 10 K/min and 20 K/min from 30 till 1100 °C. Sampling time for the µGC was set at 20 s, the temperature of modules A and B was 130 °C and 90 °C, respectively. Helium was used as the carrier gas.

2.3.3. Ash fusion temperature

For the analysis of the ash fusion behavior, three characteristic temperature points are considered: shrinkage starting temperature (SST), hemisphere temperature (HT), and flow temperature (FT). Ash samples (biomass ashed at 550 °C according to DIN EN 18122 [32], cf. section 2.3.1) were pressed into cylinders (3–4 mm in height and diameter), placed in a heating microscope (Hesse Instruments e. K., EM301) and heated up to 1600 °C. The characteristic temperature points were detected following DIN EN ISO 21404 [34].

2.4. Combustion experiments

The combustion experiments of the milled wood pellets were conducted in a PF furnace at the Institute for Energy Systems, Technical University of Munich (TUM) [35]. A schematic drawing of the reactor is shown in Fig. 1. This reactor consists of an externally heated ceramic reaction tube measuring 2000 mm in length and 144 mm in diameter. Before combustion, the tube was pre-heated to 1300 °C and kept at that temperature throughout the experiments. The (additivated) wood was then fed into the top of the tube via a vibration channel at a mass flow rate of 0.66 kg/h, corresponding to a power output of 3.2 kW (in the case of no additive).

Ash samples were collected from three locations (i.e., bottom (B), cyclone (C), and filter (F)), resulting in a total amount of 12 samples (refer to Fig. 1 for ash collection points). Table 4 provides an overview of the collected ash samples and their respective denotation.

2.4.1. Gaseous emissions

To achieve an air-fuel ratio of $\lambda = 1.2$, the air-flow (i.e., primary, secondary, and tertiary) in the reactor was adjusted to maintain an

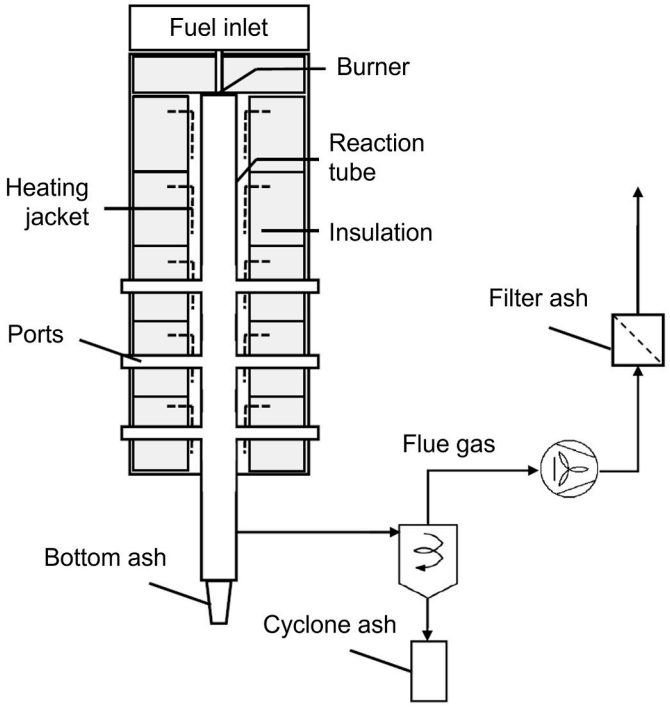

Fig. 1. Schematic set-up of pulverized fuel (PF) furnace with fuel inlet at the top and the ash collection points at the bottom (i.e., bottom, cyclone, and filter ash). Adapted from [35].

Table 4
Denotation of (with kaolin additivated) wood samples and the denotation of the collected ash fractions following the combustion trials.

Fuel	Bottom ash	Cyclone ash	Filter ash
Ref	B00	C00	F00
K05	B05	C05	F05
K10	B10	C10	F10
K15	B15	C15	F15

excess oxygen concentration of 3.5 vol%. The gas retention time was set to 5 s, while the gas analysis probe was inserted at the port at the lower end of the tube (Fig. 1), where CO_2, CO, NO, NO_2, and O_2 concentrations were recorded every 6 s (ABB AO2020 gas analyzer, calibration spans: CO_2 0–20 vol%, NO 0–1500 mg/Nm^3, NO_2 0–2500 mg/Nm^3, CO 0–10 000 vpm (volumetric parts per million), O_2 0–25 vol%).

2.4.2. Ash samples

Bottom and cyclone ash samples were collected from the trays after the combustion experiments. Filter ash was collected by scraping off the fabric filter with a spoon. To ensure sufficient amounts for subsequent chemical analysis, more specifically for IC analyses, the fabric filters were additionally rinsed with ethanol, and the washed-out ash was dried. Ignition losses from the bottom ash were determined according to DIN EN 18122 [32] at 550 °C in a muffle furnace (Nabertherm L 24/11 BO).

2.4.3. Chemical ash composition

The elemental composition of all ash samples (including K, Na, Al, Ca, Mg, and Fe) was determined via two-step acid digestion in a microwave, followed by AAS analysis (refer to section 2.3.1). Water-soluble chloride (Cl^-) and sulfate (SO_4^{2-}) ions were measured using ion chromatography (IC, Dionex Sodron ICS-90) according to DIN EN ISO 10304–1 [36].

2.4.4. Crystalline phases of bottom ash

Crystalline phase analyses of the bottom ash for the identification of reaction products from K incorporation by kaolin additivation were performed using X-ray diffraction (XRD, Siemens D500) with Cu Kα radiation at 30 mA and 40 kV. Step scanning was conducted over a range of 3°–63°, and the resulting diffractograms were analyzed using a reference database (Bruker, EVA software).

3. Results and discussion

3.1. Laboratory experiments

To investigate the potential for K retention within the bottom ash due to kaolin additivation, laboratory analyses were conducted prior to combustion experiments in the pulverized fuel furnace.

3.1.1. Water and ash content, ash and K retention

The findings obtained from the analyses of both the reference biomass and additivated biomass samples are presented in Fig. 2. The water content of the milled biomass (Ref, without additive) was 6.1 wt% and slightly lower than the 8.0 wt% of the pellets (Table 1). This difference can be attributed to the heat generated during the milling process, resulting in a water reduction of the solid biofuel. A slight increase in water content was observed with rising additive concentrations (K05, K10, K15); this is most likely due to the introduction of moisture from the additive (12 wt%, cf. Table 2). As expected, the ash content increased with rising kaolin concentrations due to the additivation of non-combustible Al-Si-based material. Ash retention expresses the amount of ash remaining after sample heating to 1100 °C, indicating the amount of (inorganic) ash compounds that do not evaporate into the gas phase at high temperatures. The potassium (K) retention expresses the relative amount of K incorporated within the ash at 1100 °C. Both retention values rise with additive content: without kaolin (Ref), 81 wt% of the total ash remained at 1100 °C, while with 1.5 wt% kaolin (K15) the retention increased to 92 wt% (Fig. 2 B, Ash retention). This rise can be attributed partly to the higher contents of Al and Si due to kaolin, leaving a higher portion of ash not evaporating into the gas phase (melting temperature of kaolin >1600 °C [37]) and partly to the incorporation of K (and other alkali metals, such as Na) into compounds with high melting temperatures, such as kalsilite ($KAlSiO_4$, T_{melt} > 1600 °C) and leucite ($KAlSi_2O_6$, T_{melt} > 1500 °C) [6]. The incorporation of K is also reflected in the K retention (Fig. 2 B, K retention): for samples without additive (Ref), the K retention is at 34 wt% but increases to 86, 92, and 96 wt% with 0.5, 1.0, and 1.5 wt% kaolin (K05, K10, K15), respectively.

3.1.2. Gas evolution from thermal degradation

The results of the measurements of the gas evolved during thermogravimetric analyses experiments of the four (additivated) biomass samples, expressed as the molar CO/CO_2 ratios, are shown in Fig. 3. Additionally, the respective weight-loss curves and the first derivatives (DTG curves) of these biomass samples and kaolin as a reference are presented. The results corresponding to a heating rate of 10 K/min are shown in the left column, whereas those for 20 K/min are displayed in the right column.

The weight loss curve for the biomass samples can be subdivided into three stages: from 30 to ca. 200 °C, from 200 to 370 °C, and from 370 up to 600 °C. For both heating rates, three DTG peaks can be observed. However, at the higher heating rate of 20 K/min, these peaks show a slight shift toward elevated temperatures. These three DTG peaks correspond to the evaporation of moisture from the samples, the release of volatile components mainly originating from holocellulose and partial lignin decomposition, and the combustion of the remaining lignin and char, respectively [38].

Kaolin exhibits a characteristic mass loss peak around 550 °C, which can be attributed to phase changes and dehydroxylation (equation (1),

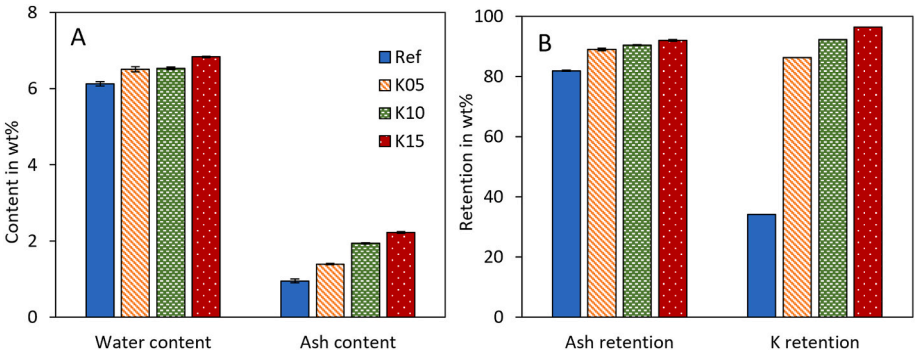

Fig. 2. Laboratory analyses of non-additivated (Ref) and additivated fuel samples (K05-K15: 0.5-1.5 wt% kaolin). **A** Water and ash content, **B** ash and potassium (K) retention of samples heated at 1 100 °C compared to 550 °C.

section 1).

Regarding the molar CO/CO_2 ratios observed for the biomass samples, two notable maxima appear. The first maximum correlates with the first DTG peak, while the second peak or shoulder corresponds to the third local maximum in the DTG curve. At a heating rate of 20 K/min, these maxima are spread over a wider temperature range, whereas at 10 K/min they are narrower. Above 600 °C, the CO/CO_2 ratio at specific measurement points decreases to zero. This behavior is attributed to the overall low release of CO and CO_2 in this temperature range, where some CO concentrations fall below the detection threshold.

When considering the additivated samples heated at 20 K/min, the third DTG maximum appears slightly broader. Specifically, the peak ends at about 580 °C in the reference biomass sample (20 K/min, Ref), whereas it extends beyond 600 °C in the presence of 1.5 wt% kaolin (20 K/min, K15). This effect is likely due to the mass loss associated with kaolin present in the samples up to ca. 700 °C. Furthermore, for both heating rates (10 and 20 K/min), the second shoulder peak in the CO/CO_2 ratio decreases upon kaolin additivation. This observation suggests either a reduced relative release of CO compared to CO_2 from the biomass or an enhanced oxidation of CO to CO_2 following its release, oxidizing prior to measurement in the micro gas chromatograph (μGC). This can be attributed to the fact that at temperatures above 450 °C, where the second peak in the CO/CO_2 ratio is observed, kaolin undergoes phase transformations leading to the formation of its reactive phase, meta-kaolin. Meta-kaolin can then react with KOH and KCl, binding these species in the ash and thereby preventing them from inhibiting the oxidation of CO to CO_2.

The trends described above align with research findings showing the mitigation of CO emissions with the additivation of kaolin during the combustion of solid biomass [14–16], indicating the potential of kaolin in these concentrations to mitigate CO emissions in pulverized fuel furnaces.

3.1.3. Ash fusion temperatures

The presence of K in biomass ashes not only contributes to the formation of inorganic particulate matter (PM) emissions and increased CO emissions due to incomplete combustion [16] but also leads to the formation of K-Si compounds with low melting temperatures (T_{melt}). This reduces ash fusion temperatures, increasing the risk of slagging in combustion furnaces. With kaolin, reactions bind K (and Si) as K-Al-silicates with high melting temperatures, which can mitigate slagging issues. The results in Fig. 4 demonstrate this behavior: shrinkage starting temperature (SST), hemisphere temperature (HT), and flow temperature (FT) increased with increasing kaolin concentrations, indicating the formation of the K-Al-silicates as mentioned above. With the additivation of 1.5 wt% kaolin (K15), the ash fusion temperatures rose to 1273 °C (SST), 1326 °C (HT), and 1432 °C (FT).

3.2. Combustion experiments

Following the laboratory experiments, combustion tests were conducted in the PF furnace.

3.2.1. Gaseous emissions

Fig. 5 presents the gaseous emissions (i.e., CO, CO_2, NO, and NO_2, also cumulated in NO_x, as well as O_2), along with the fuel mass input and relative reactor pressure during the combustion of the additivated wood (K05, K10, K15) and the reference fuel. The data include emissions during the respective experimental duration (Table 5), but have been cleaned to exclude periods without fuel supply due to solid bridges.

- The CO emissions demonstrated significant fluctuations, reaching levels of up to 23 000 vpm, often exceeding calibration spans. The absolute values are thus to be regarded as only conditionally reliable. Overall, no apparent differences were observed between the reference and additive cases. These high emissions suggest incomplete combustion, which can only partly be attributed to the position of the measurement probe in the lower quarter of the reactor rather than in the exhaust channel. The ash analysis provides further confirmation of incomplete combustion (i.e., bottom ash, section 3.2.3).
- Regarding CO_2 emissions, the reference case (Ref, wood without additive) exhibited a higher median concentration of 11.7 vol% than the additivated samples. The median concentrations of the cases with 1.0 and 1.5 wt% kaolin were nearly the same (10.4 and 10.2 vol% for K10 and K15, respectively), while CO_2 concentrations for the 0.5 wt % case (K05) fluctuated considerably (median: 11.1 vol%). The lower CO_2 concentrations in the additivated cases may be due to dilution from increased O_2 levels.
- During the combustion of the reference material, lower O_2 levels than during the combustion of additivated fuels were measured. Although the air-flow was set at 3.5 vol% O_2 for the targeted $\lambda = 1.2$, the median concentrations reached 3.1, 4.3, 4.4, and 4.2 vol% O_2 for Ref, K05, K10, and K15, respectively. With similar air-flows, this difference could be attributed to two potential mechanisms: (1) dilution of combustibles within the fuel due to the additive, reducing overall O_2 consumption, or (2) inhibition of oxidation by the additive. The inhibition effect may result from the endothermal conversion of kaolin into meta-kaolin, which locally reduces the temperatures required for complete combustion. Additionally, diffusion limitations could have occurred due to the coverage of wood particles with kaolin, further hindering oxidation. However, the limited residence time in the reactor did not compensate for this effect. In grate-bed firing systems, kaolin additivation has typically improved oxidation conditions, leading to lower CO emissions, while reported O_2 levels remained largely unaffected [10,15,21,39].
- NO_x emissions (also shown separately as NO and NO_2 in Fig. 5) also exhibited high variability, with a tendency for increased

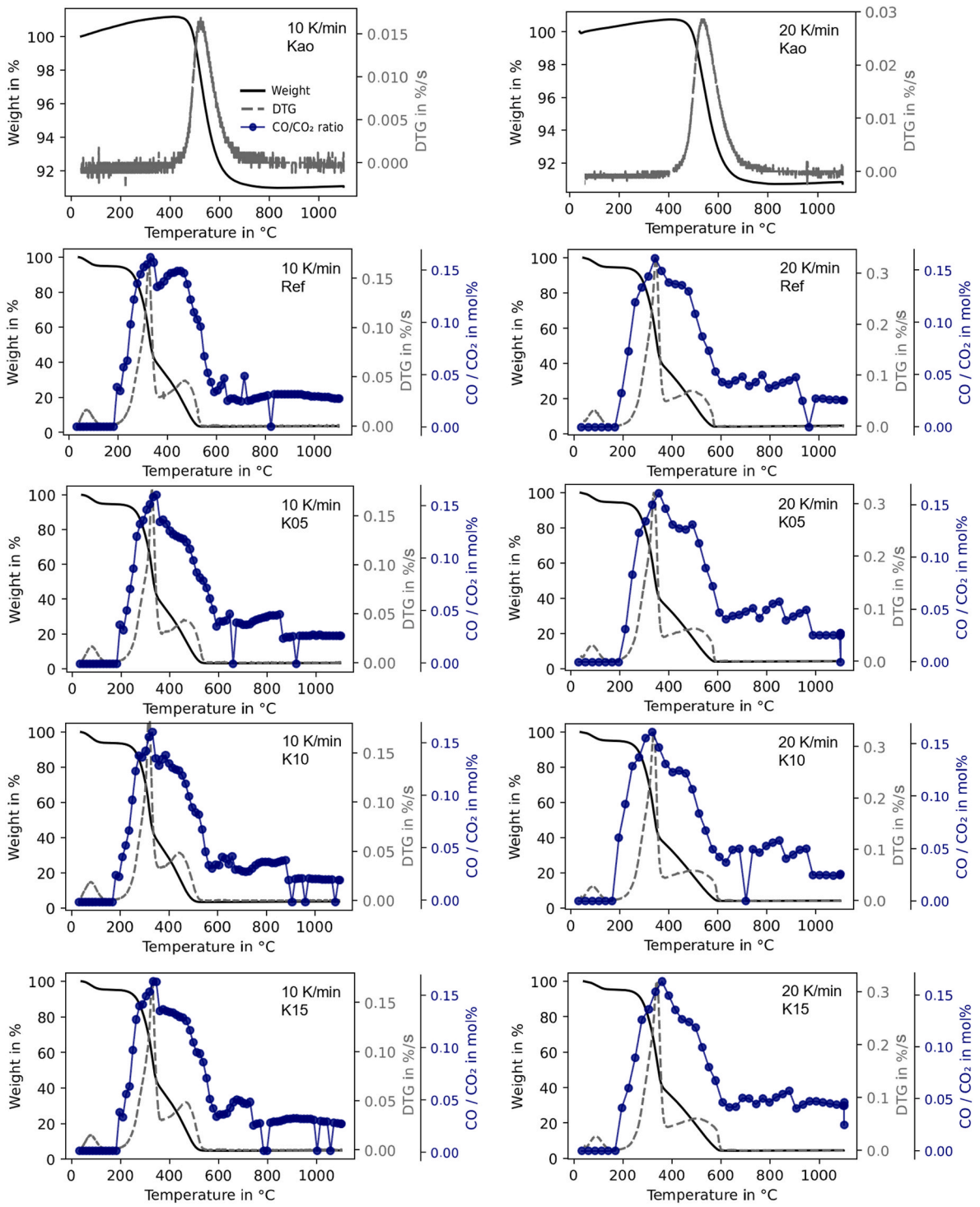

Fig. 3. Weight loss curves, the first derivative of the weight loss (DTG), and the CO/CO_2 ratio during TGA experiments from 30 till 1 100 °C with a heating rate of 10 K/min (left column) and 20 K/min (right column) for Kaolin (Kao, only weight loss), non-additivated (Ref) and additivated (K05, K10, K15: 0.5, 1.0, 1.5 wt% kaolin) pulverized wood pellets.

concentrations in the additive samples. However, when normalizing CO emissions to a uniform O_2 content, the additivated fuels appear to exhibit higher CO emissions compared to the reference. This contradicts the expected trend, as NO_x emissions usually correlate inversely with CO emissions: both are oxidation products of nitrogen and carbon from biomass, with NO_x as a final oxidation product and CO as an intermediate that can further oxidize to CO_2 [40]. Typically, decreasing CO emissions correspond to increasing NO_x emissions, but this relationship is not evident in the present case.

Overall, these data indicate that the PF system was operated far from equilibrium, likely due to insufficient residence time for wood particles and gases within the reactor. This limits the conclusions that can be drawn for the influence of kaolin additivation on gaseous emissions in PF furnaces and underscores the need for deeper investigation under

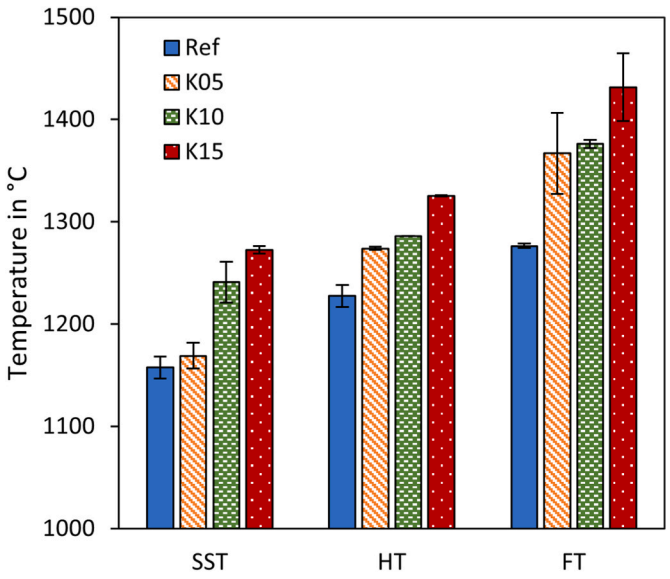

Fig. 4. Ash fusion behavior of non-additivated (Ref) and additivated fuel samples (K05, K10, K15: 0.5, 1.0, 1.5 wt% kaolin) according to DIN EN ISO 21404 [34] (SST shrinkage starting temperature, HT hemisphere temperature, FT flow temperature).

more controlled, steady-state conditions. Measures to enhance complete burnout could include reducing air velocity and reducing particle size to increase particle residence time in the reactor.

3.2.2. Ash samples

The masses of the collected ash samples from the respective combustion experiments in the PF furnace are summarized in Table 5. For filter ashes, only the scraped ashes are considered here, while the ethanol-rinsed amounts were used only for IC analyses. Due to the plant's geometric design and ash losses between connecting lines of the different ash collection points, a complete elemental balance of the ash input and output streams is not possible, and the ash collection weights are only considered as indicative trends for the respective collection

Table 5
Ash sample collection weights from combustion experiments in pulverized fuel (PF) furnace with non-additivated (Ref) and additivated wood (K05, K10, K15: 0.5, 1.0, 1.5 wt% kaolin).

Fuel	Duration of experiment hh:mm:ss	Ash weight at collection in g		
		Bed ash (B)	Cyclone ash (C)	Filter ash (F)
Ref	04:25:28	12.6	0.8	0.2
K05	03:40:15	10.5	2.1	1.5
K10	02:48:16	8.7	0.8	0.2
K15	02:53:35	9.8	2.4	0.3

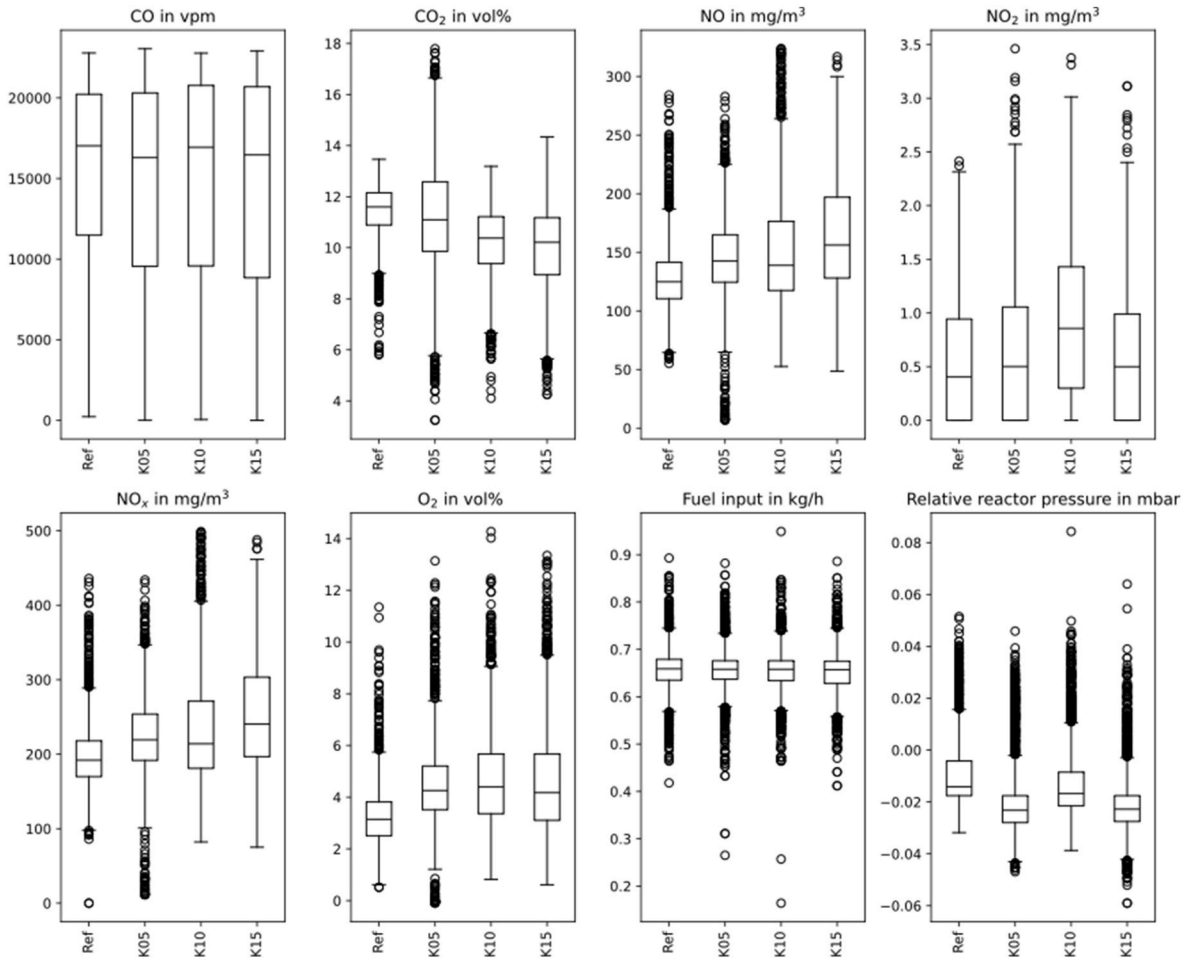

Fig. 5. Boxplots of gaseous emission (CO, CO_2, NO, NO_2, NO_x, O_2), fuel input, and reactor pressure during the combustion of non-additivated (Ref) and additivated (K05, K10, K15: 0.5, 1.0, 1.5 wt% kaolin) pulverized wood pellets in a pulverized fuel (PF) furnace. Boxes span from quartile 25 % (Q1) to 75 % (Q3) (interquartile-range IQR), line marks median, dots show outliers, whiskers cover the range of accepted values, reaching from box to datapoints within 1.5IQR: (minimum value without outliers < Q1–1.5xIQR, maximum value without outliers > Q3 + 1.5xIQR).

points. Aside from increased bottom ash sample weight with longer experiment durations, no clear trend is observed in the cyclone and filter ash collection weights. Compared to the reference (Ref) and C10 samples, the cyclone collection weights for C05 and C15 are approx.three times higher than those of the reference fuel. The filter ash amount represents only the material scraped off the fabric filter with a spoon (i.e., excluding the washed-out fraction with ethanol, refer to section 2.4.2). Notably, the collected filter ash for F05 stands out with 1.5 g, significantly higher than the 0.2 to 0.3 wt% recorded for Ref, F10, and F15. This suggests that larger ash particles may have been entrained into the flue gas system, reaching the fabric filter in greater quantities.

The ignition losses (Table 6) indicate high amounts of unburned fuel, ranging between 70 and 80 %. One possible explanation is that the median particle size of the fuel was too small, leading to insufficient retention time for the larger fuel particles within the reactor, preventing complete combustion.

3.2.3. Chemical composition of ashes

No conclusive trends were observed regarding the chemical composition of the bottom ashes from the PF furnace combustion trials (Fig. 6). The concentrations of key elements (i.e., K, Na, Al, Ca, Mg, Fe, Cl^-, SO_4^{2-}, Mn, Zn, Cu, Cr, Ni, and Cd) were generally low (e.g., 7 to 10 mg_K/g_{ash}, <2.8 mg_{Na}/g_{ash}, 2 to 6 mg_{Al}/g_{ash}, 11 to 22 mg_{Ca}/g_{ash}) and exhibited high standard deviations, which makes the data insufficiently reliable. These variations are likely connected to the ignition losses due to incomplete burnout, as depicted in Table 6 and discussed in section 3.2.1.

In the case of the cyclone ash, K fractions were higher in C05 and C15 (i.e., 99 and 118 mg_K/g_{ash}, respectively), whereas C10 (81 mg_K/g_{ash}) had slightly lower values than the reference case (88 mg_K/g_{ash}). The relatively large amounts of C05 and C15 collected (Table 5) suggest either that bottom ash was carried over into the flue gas system (as the cyclone was positioned at a similar height to the bed ash container) or that more additive-derived reaction products were sequestered in the cyclone. This is reflected in the increased K concentrations, while Ca, Mg, and Fe levels remained nearly unchanged. However, no significant rise in aluminum concentrations was observed, which would indicate the accumulation of kaolin or K-Al-Si compounds. Given that the sum of detected species accounted for only <350 mg/g_{ash} (or < 470 mg/g_{ash} when expressed as oxides), the presence of undefined components such as Si, P, and unburned material could have contributed to dilution effects [18,22]. Further analyses were not possible due to low remaining sample sizes. For C10, only a small amount of ash was collected, and some material was lost during shipment, leading to gaps in the IC analysis results (i.e., Cl^- and SO_4^{2-}).

The ashes from the fabric filters showed a slight trend of decreasing K with increasing additive (116, 94, 82, and 104 mg_K/g_{ash} for F00, F05, F10, and F15, respectively). The highest ash masses were collected for F05 and F15 (Table 5), also considering the duration of the respective combustion experiments. Notably, the collected filter ash for F05 stands out with 1.5 g, significantly higher than the 0.2 to 0.3 wt% recorded for Ref, F10, and F15. This suggests that larger ash particles may have been entrained into the flue gas system, reaching the fabric filter in greater quantities. Here, Ca emissions were significantly higher (151 and 117 mg_{Ca}/g_{ash} for F05 and F15, respectively) compared to F00 and F10 (88 and 81 mg_{Ca}/g_{ash}, respectively). A similar trend was observed for Cl^- and SO_4^{2-}.

The decrease of K in the filter ash generally complies with studies in literature, reporting alkali-capture by additives and thereby lowering of particle formation (e.g., with coal fly ash [12,17,18]).

No substantial trends were evident for trace metals (Mn, Zn, Cu, Cr, Ni, and Cd). Cd, Ni, Cr, and Cu remained close to or below detection limits. For filter ash, Zn concentrations were highest in F00 (39 mg_{Zn}/g_{ash}) and decreased with the additive content. One possible explanation is related to ZnO's vapor pressure and its interaction with lower-melting-point K compounds such as KCl or K_2SO_4. With less KCl and K_2SO_4 present (e.g., due to kaolin additivation), fewer condensable species may have adhered to ZnO particles, reducing their size and making them less likely to be retained by the fabric filter [41]. Mn concentrations in the filter ash (2.1, 4.3, 2.3, and 2.9 mg_{Mn}/g_{ash} for F00-F15, respectively) were comparable to the cyclone ashes, with the highest concentration observed in F05, which had the largest total ash mass. No evident influence of the additive on Mn concentrations was observed here.

3.2.4. Crystalline phases of bottom ash

X-ray diffraction (XRD) analyses were conducted for the bottom ashes (B00-B15), as displayed in Fig. 7, with a focus on identifying phases related to kaolin reaction pathways and K incorporation (i.e., K-Al-Si-compounds). The diffractograms indicate a significant presence of amorphous material and carbon residues, as evidenced by background noise in the signals. SiO_2 was detected in all bottom ashes, while peaks corresponding to K-Al-Si reaction products—such as orthoclase ($KAlSi_3O_8$), leucite ($KAlSi_2O_6$), and kalsilite ($KAlSiO_4$)—became visible with kaolin additivation of ≥0.5 wt%. In the case of B15, muscovite ($KAl_2Si_3AlO_{10}(OH)_2$) was also detected. According to De Riese et al. [42], the ability of kaolin to capture potassium decreases with increasing temperature, as compounds like kalsilite ($KAlSiO_4$) become less stable at higher temperatures. This could explain why $KAlSi_3O_8$ was detected in all bottom ash samples here, whereas $KAlSiO_4$ is more commonly found in grate-bed combustion systems, where temperatures are typically lower [20]. Overall, the results from XRD analyses confirm the reactions of K with kaolin and its incorporation into the bottom ashes, even though the elemental analysis of the ashes (Fig. 6) did not exhibit a rise in total concentrations of K with additive content in the fuel.

Table 6
Ignition losses of bed ash ($n = 5$) from combustion experiments in pulverized fuel (PF) furnace with non-additivated (B00) and additivated wood (B05, B10, B15: wood with 0.5, 1.0, 1.5 wt% kaolin).

Bed ash	Ignition losses in wt%
B00	75.4 ± 16.0
B05	72.4 ± 14.3
B10	82.0 ± 8.1
B15	85.0 ± 8.8

4. Conclusions

The present study demonstrates that in laboratory conditions, kaolin additivation significantly enhances potassium retention within the ash and increases ash fusion temperatures. Namely, the potassium retention rose from 34 % in the non-additivated reference fuel to up to 96 % in samples with the highest additive concentration of 1.5 wt% kaolin, correlating with increased ash fusion temperatures—shrinkage starting temperature (SST), hemisphere temperature (HT), and flow temperature (FT) increased up to 1273 °C, 1326 °C, and 1432 °C. In pulverized biomass combustion systems, this suggests a reduction in the release of volatile potassium species.

Combustion experiments carried out in a PF furnace revealed that despite the promising ash chemistry modifications and the formation of stable potassium-aluminosilicate compounds in the bottom ashes, such as kalsilite ($KAlSiO_4$), leucite ($KAlSi_2O_6$), and orthoclase ($KAlSi_3O_8$), identified using X-ray diffraction, the overall combustion efficiency in this present study was limited by incomplete burnout. This was evidenced by high CO emissions of up to 23 000 vpm and substantial ignition losses in bottom ash (up to 85 wt%). Furthermore, gaseous emission measurements indicated no significant reduction in CO emissions between the reference and additivated samples, and some variation in NO_x emissions, also suggesting that combustion reactions were far from equilibrium. This limits the conclusions that can be drawn for the influence of kaolin additivation on gaseous emissions in PF furnaces

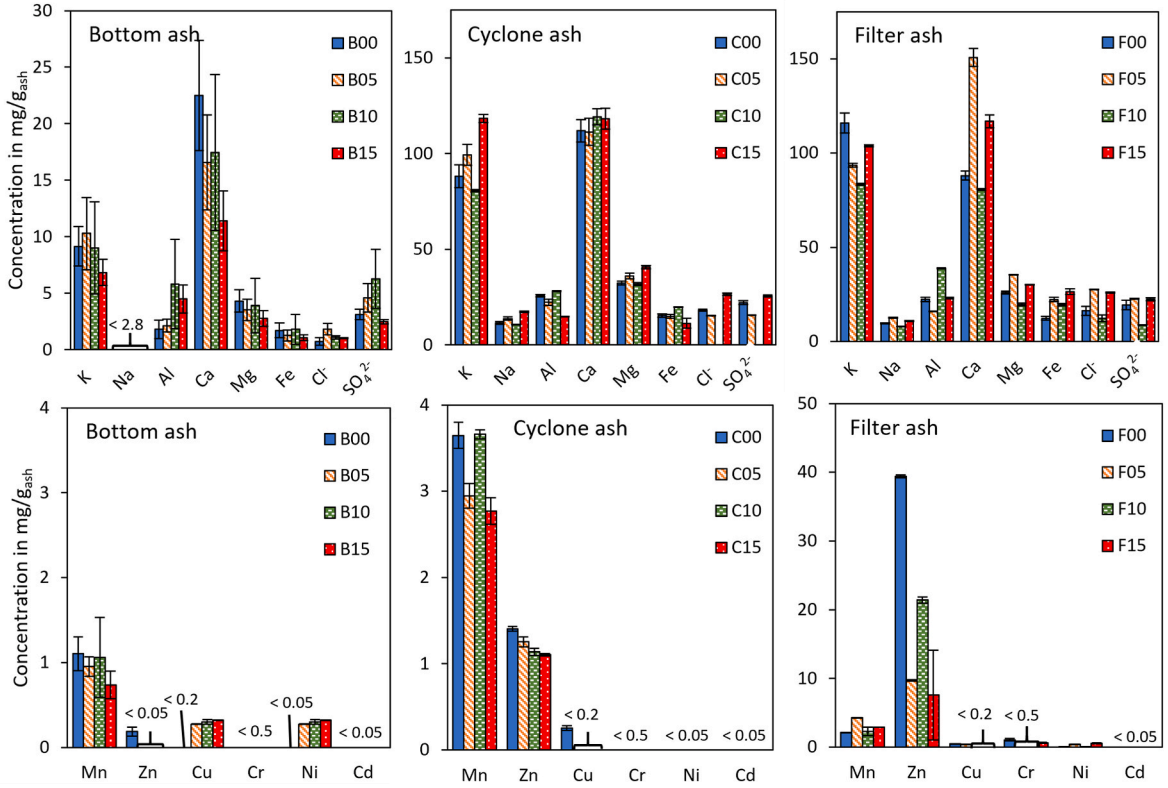

Fig. 6. Chemical analysis of ashes from the combustion of non-additivated and additivated wood in a pulverized fuel (PF) furnace. The letters indicate the ash fraction of bottom (B), cyclone (C), and filter (F) ash, while the numbers represent the amount of additive content (00-15: 0.0 – 1.5 wt% additive).

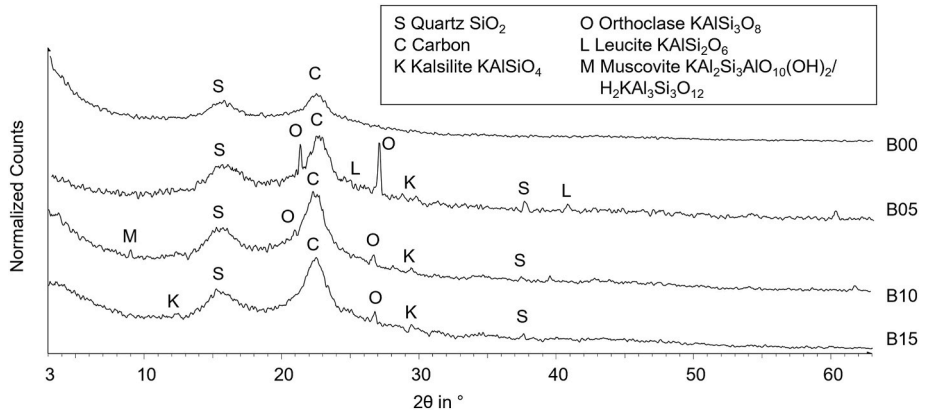

Fig. 7. X-Ray diffractograms of bottom ashes and associated phases from the combustion of non-additivated (B00) and additivated (B05-B15) wood in a (PF) furnace.

and underscores the need for deeper investigation under more controlled, steady-state conditions. This incomplete combustion was likely due to insufficient residence time and suboptimal particle size distributions in the laboratory reactor, resulting in limited oxidation of the fuel particles. Specifically, adjusting furnace conditions—such as increasing gas and particle residence times—by reducing the particle size of the pulverized biomass feed needs to be aligned to enhance burnout.

The comparative evaluation across scales demonstrates that under laboratory conditions, the potential of kaolin to bind potassium into temperature-stable compounds was clearly demonstrated, while corresponding trends were also observed in the pilot-scale furnace. An evaluation of the full benefits of kaolin additivation in PF furnaces – particularly in terms of emission mitigation – can only be fully realized when fuel properties and furnace operation are jointly optimized.

CRediT authorship contribution statement

Theresa Siegmund: Writing – original draft, Visualization, Methodology, Investigation, Conceptualization. **Marvin Scherzinger:** Writing – review & editing, Supervision. **Martin Kaltschmitt:** Writing – review & editing, Supervision.

Funding

Part of this work was financed by a study conducted for Hamburger Energiewerke GmbH. Publishing fees were supported by Funding Program Open Access Publishing of Hamburg University of Technology (TUHH).

Declaration of competing interest

The authors declare no conflict of interest.

Data availability

Data will be made available on request.

References

[1] J.P. Wolf, Dong, biomass combustion for power generation: an introduction, in: Biomass Combustion Science, Technology and Engineering, Elsevier, 2013, pp. 3–8, https://doi.org/10.1533/9780857097439.1.3.

[2] Y. Niu, H. Tan, S. Hui, Ash-related issues during biomass combustion: Alkali-induced slagging, silicate melt-induced slagging (ash fusion), agglomeration, corrosion, ash utilization, and related countermeasures, Prog. Energy Combust. Sci. 52 (2016) 1–61, https://doi.org/10.1016/j.pecs.2015.09.003.

[3] M. Kieltyka, A.P. Soares Dias, H. Kubiczek, B. Sarapata, T. Grzybek, The influence of poisoning on the deactivation of DeNOx catalysts, comptes rendus, Chimie 18 (2015) 1036–1048, https://doi.org/10.1016/j.crci.2015.05.004.

[4] L. Schill, R. Fehrmann, Strategies of coping with deactivation of NH3-SCR catalysts due to biomass firing, Catalysts 8 (2018) 135, https://doi.org/10.3390/catal8040135.

[5] H. Wu, G. Wang, P.A. Jensen, F. Jappe Frandsen, P. Glarborg, Reactive Additives for Alkali Capture in Biomass Combustion, 2018.

[6] G. Wang, P.A. Jensen, H. Wu, F.J. Frandsen, B. Sander, P. Glarborg, Potassium capture by Kaolin, part 1: KOH, Energy Fuel. 32 (2018) 1851–1862, https://doi.org/10.1021/acs.energyfuels.7b03645.

[7] H. Mörtenkötter, M. Kulkarni, L. Fuchs, F. Kerscher, S. Fendt, H. Spliethoff, Effects of aluminosilicate-based additives on potassium release and ash melting during biomass combustion, Fuel 374 (2024) 132471, https://doi.org/10.1016/j.fuel.2024.132471.

[8] R. Mack, C. Schön, D. Kuptz, H. Hartmann, T. Brunner, I. Obernberger, H.M. Behr, Influence of wood species and additives on emission behavior of wood pellets in a residential pellet stove and a boiler, Biomass Convers. Biorefinery (2023), https://doi.org/10.1007/s13399-023-04204-x.

[9] J.L. Míguez, J. Porteiro, F. Behrendt, D. Blanco, D. Patiño, A. Dieguez-Alonso, Review of the use of additives to mitigate operational problems associated with the combustion of biomass with high content in ash-forming species, Renew. Sustain. Energy Rev. 141 (2021) 110502, https://doi.org/10.1016/j.rser.2020.110502.

[10] L.S. Bäfver, M. Rönnbäck, B. Leckner, F. Claesson, C. Tullin, Particle emission from combustion of oat grain and its potential reduction by addition of limestone or kaolin, Fuel Process. Technol. 90 (2009) 353–359, https://doi.org/10.1016/j.fuproc.2008.10.006.

[11] W. Cheng, Y. Zhu, J. Shao, W. Zhang, G. Wu, H. Jiang, J. Hu, Z. Huang, H. Yang, H. Chen, Mitigation of ultrafine particulate matter emission from agricultural biomass pellet combustion by the additive of phosphoric acid modified kaolin, Renew. Energy 172 (2021) 177–187, https://doi.org/10.1016/j.renene.2021.03.041.

[12] A. Fuller, Y. Omidiji, T. Viefhaus, J. Maier, G. Scheffknecht, The impact of an additive on fly ash formation/transformation from wood dust combustion in a lab-scale pulverized fuel reactor, Renew. Energy 136 (2019) 732–745, https://doi.org/10.1016/j.renene.2019.01.013.

[13] N. Nor Aznizam Nik Norizam, J. Szuhánszki, I. Ahmed, X. Yang, D. Ingham, K. Milkowski, A. Gheit, A. Heeley, L. Ma, M. Pourkashanian, Impact of the blending of kaolin on particulate matter (PM) emissions in a biomass field-scale 250 kW grate boiler, Fuel 374 (2024) 132454, https://doi.org/10.1016/j.fuel.2024.132454.

[14] R. Mack, D. Kuptz, C. Schön, H. Hartmann, Combustion behavior and slagging tendencies of kaolin additivated agricultural pellets and of wood-straw pellet blends in a small-scale boiler, Biomass Bioenergy 125 (2019) 50–62, https://doi.org/10.1016/j.biombioe.2019.04.003.

[15] M. Gehrig, M. Wöhler, S. Pelz, J. Steinbrink, H. Thorwarth, Kaolin as additive in wood pellet combustion with several mixtures of spruce and short-rotation-coppice willow and its influence on emissions and ashes, Fuel 235 (2019) 610–616, https://doi.org/10.1016/j.fuel.2018.08.028.

[16] T. Siegmund, C. Gollmer, M. Scherzinger, M. Kaltschmitt, A review of CO emissions during solid biofuel combustion – formation mechanisms and fuel-related reduction measures, J. Energy Inst. 116 (2024) 101762, https://doi.org/10.1016/j.joei.2024.101762.

[17] R. Nowak Delgado, T. De Riese, P. Johne, S. Fendt, H. Spliethoff, Impact of coal fly ash addition on combustion aerosols ($PM_{2.5}$) in Pilot- and full-scale pulverized wood combustion: a comparative Study, Energy Fuel. 36 (2022) 13665–13677, https://doi.org/10.1021/acs.energyfuels.2c02763.

[18] H. Wu, M.S. Bashir, P.A. Jensen, B. Sander, P. Glarborg, Impact of coal fly ash addition on ash transformation and deposition in a full-scale wood suspension-firing boiler, Fuel 113 (2013) 632–643, https://doi.org/10.1016/j.fuel.2013.06.018.

[19] A.J. Damoe, H. Wu, F.J. Frandsen, P. Glarborg, B. Sander, Impact of coal fly ash addition on combustion aerosols ($PM_{2.5}$) from full-scale suspension-firing of pulverized wood, Energy Fuel. 28 (2014) 3217–3223, https://doi.org/10.1021/ef5003815.

[20] T. Siegmund, C. Gollmer, N. Horstmann, M. Kaltschmitt, Carbon monoxide (CO) and particulate matter (PM) emissions during the combustion of wood pellets in a small-scale combustion unit – influence of aluminum-(silicate-)based fuel additivation, Fuel Process. Technol. (2024), https://doi.org/10.1016/j.fuproc.2024.108111.

[21] C. Gollmer, T. Siegmund, V. Weigel, M. Kaltschmitt, Comparative analysis of primary and secondary emission mitigation measures for small-scale wood chip combustion, Energies 17 (2024) 4403, https://doi.org/10.3390/en17174403.

[22] K.O. Davidsson, L.-E. Åmand, A.-L. Elled, B. Leckner, Effect of cofiring coal and biofuel with sewage sludge on alkali problems in a circulating fluidized bed boiler, Energy Fuel. 21 (2007) 3180–3188, https://doi.org/10.1021/ef700384c.

[23] C. Fütterer, A. Stahl, Elementbestimmung Mit ICP-OES M02.015.03, Hamburg: Technische Universität Hamburg, Zentrallabor Chemische Analytik, 2020.

[24] H. Cöllen, H. Frerichs, A. Stahl, Elementbestimmung per ICP-MS, M02.013.01, Hamburg: Technische Universität Hamburg, Zentrallabor Chemische Analytik, 2022.

[25] H. Diedrich, A. Stahl, H. Frerichs, NCHS-Elementaranalyse M02.001.02, Hamburg: Technische Universität Hamburg, Zentrallabor Chemische Analytik, 2022.

[26] National Center for Biotechnology Information, Compound Summary for CID 92024769, Kaolin, PubChem, n.d. https://pubchem.ncbi.nlm.nih.gov/compound/92024769. (accessed February 19, 2025).

[27] Gebrüder Dorfner GmbH & Co. Kaolin- Und Kristallquarzsandwerke KG, Kaolin Composition, (n.d.).

[28] S.V. Vassilev, D. Baxter, C.G. Vassileva, An overview of the behaviour of biomass during combustion: part II. Ash fusion and ash formation mechanisms of biomass types, Fuel 117 (2014) 152–183, https://doi.org/10.1016/j.fuel.2013.09.024.

[29] T.R. Miles, T.R. Miles, L.L. Baxter, R.W. Bryers, B.M. Jenkinsq, S.W. Arrowwood, Boiler Deposits from Firing Biomass Fuels, 1996.

[30] S.V. Vassilev, D. Baxter, C.G. Vassileva, An overview of the behaviour of biomass during combustion: part I. Phase-mineral transformations of organic and inorganic matter, Fuel 112 (2013) 391–449, https://doi.org/10.1016/j.fuel.2013.05.043.

[31] L. Wang, J.E. Hustad, Ø. Skreiberg, G. Skjevrak, M. Grønli, A critical review on additives to reduce ash related operation problems in biomass combustion applications, Energy Proc. 20 (2012) 20–29, https://doi.org/10.1016/j.egypro.2012.03.004.

[32] DIN EN ISO 18122 Solid Biofuels Determination of Ash Content, 2015.

[33] Deutsches Institut für Normungen e.V., DIN 22022-1 solid fuels – determination of contents of trace elements – part 1: general rules, sampling and sample preparation – preparation of samples for the analyses. Dissolution Method), 2014.

[34] Deutsches Institut für Normungen e.V., DIN EN ISO 21404: Solid Biofuels – Determination of Ash Melting Behaviour, 2020.

[35] C. Wolf, T.J. Leino, A.R. Stephan, M.J. Aho, H. Spliethoff, Online corrosion measurements in combination with deposit and aerosol analysis during the Co-firing of straw with coal in electrically heated, small-scale pulverized fuel and circulating fluidized bed systems, Energy Fuel. 32 (2018) 2506–2516, https://doi.org/10.1021/acs.energyfuels.7b03976.

[36] DIN EN ISO 10304-1 Water Quality – Determination of Dissolved Anions by Liquid Chromatography of Ions – Part 1: Determination of Bromide, Chloride, Fluoride, Nitrate, Nitrite, Phosphate and Sulfate, n.d.

[37] H.K. Nguyen, J.H. Moon, S.H. Jo, S.J. Park, D.H. Bae, M.W. Seo, H.W. Ra, S.-J. Yoon, S.-M. Yoon, J.G. Lee, T.-Y. Mun, B. Song, Ash characteristics of oxy-biomass combustion in a circulating fluidized bed with kaolin addition, Energy 230 (2021) 120871, https://doi.org/10.1016/j.energy.2021.120871.

[38] J.-J. Lu, W.-H. Chen, Investigation on the ignition and burnout temperatures of bamboo and sugarcane bagasse by thermogravimetric analysis, Appl. Energy 160 (2015) 49–57, https://doi.org/10.1016/j.apenergy.2015.09.026.

[39] S. Xiong, J. Burvall, H. Örberg, G. Kalen, M. Thyrel, M. Öhman, D. Boström, Slagging characteristics during combustion of corn stovers with and without kaolin and calcite, Energy Fuel. 22 (2008) 3465–3470, https://doi.org/10.1021/ef700718j.

[40] M. Cardu, M. Baica, Regarding the relation between the NOx content and CO content in thermo power plants flue gases, Energy Convers. Manag. 46 (2005) 47–59, https://doi.org/10.1016/j.enconman.2004.02.009.

[41] T. Hülsmann, V. Kovač, Feinstaubemissionen Bei Der Verbrennung Von Holz- Und Holz/Stroh-Mischpellets: Einfluss Einer Brennstoffadditivierung, Verlag Dr. Kovač, 2019.

[42] T. De Riese, S. Fendt, H. Spliethoff, Utilising thermodynamic equilibrium calculations to model potassium capture by aluminosilicate additives in biomass combustion plants, Fuel 340 (2023) 127591, https://doi.org/10.1016/j.fuel.2023.127591.